PNAS RESEARCH ARTICLE | NEUROSCIENCE OPEN ACCESS

The evolutionarily conserved miRNA-137 targets the neuropeptide hypocretin/orexin and modulates the wake to sleep ratio

Anja Holm[a,b,1,2], Marie-Laure Possovre[c,2], Mojtaba Bandarabadi[c], Kristine F. Moseholm[a,d], Jessica L. Justinussen[e], Ivan Bozic[f,g], René Lemcke[e], Yoan Arribat[c], Francesca Amati[c], Asli Silahtaroglu[h], Maxime Juventin[i], Antoine Adamantidis[f,g], Mehdi Tafti[c,3], and Birgitte R. Kornum[a,e,3]

Edited by Joseph Takahashi, The University of Texas Southwestern Medical Center, Dallas, TX; received July 5, 2021; accepted March 2, 2022

Hypocretin (Hcrt), also known as orexin, neuropeptide signaling stabilizes sleep and wakefulness in all vertebrates. A lack of Hcrt causes the sleep disorder narcolepsy, and increased Hcrt signaling has been speculated to cause insomnia, but while the signaling pathways of Hcrt are relatively well-described, the intracellular mechanisms that regulate its expression remain unclear. Here, we tested the role of microRNAs (miRNAs) in regulating Hcrt expression. We found that miR-137, miR-637, and miR-654-5p target the human *HCRT* gene. miR-137 is evolutionarily conserved and also targets mouse *Hcrt* as does miR-665. Inhibition of miR-137 specifically in Hcrt neurons resulted in Hcrt upregulation, longer episodes of wakefulness, and significantly longer wake bouts in the first 4 h of the active phase. IL-13 stimulation upregulated endogenous miR-137, while *Hcrt* mRNA decreased both in vitro and in vivo. Furthermore, knockdown of miR-137 in zebrafish substantially increased wakefulness. Finally, we show that in humans, the *MIR137* locus is genetically associated with sleep duration. In conclusion, these results show that an evolutionarily conserved miR-137:Hcrt interaction is involved in sleep–wake regulation.

sleep | wake | miR-137 | hypocretin | orexin

Significance

The hypocretin (Hcrt, also known as orexin) neuropeptides regulate sleep and wake stability, and disturbances of Hcrt can lead to sleep disorders. MicroRNAs (miRNAs) are short noncoding RNAs that fine-tune protein expression levels, and miRNA-based therapeutics are emerging. We report a functional interaction between miRNA (miR-137) and *Hcrt*. We demonstrate that intracellular miR-137 levels in Hcrt neurons regulate *Hcrt* expression with downstream effects on wakefulness. Specifically, lowering of miR-137 levels increased wakefulness in mice. We further show that the miR-137:Hcrt interaction is conserved across mice and humans, that miR-137 also regulates sleep–wake balance in zebrafish, and that the *MIR137* locus is genetically associated with sleep duration in humans. Together, our findings reveal an evolutionarily conserved sleep–wake regulatory role of miR-137.

Hypocretins (Hcrts), also known as orexins, are hypothalamic neuropeptides essential for the proper regulation of vigilance states. The hypocretin neuropeptide precursor (HCRT) and its peptide products hypocretin-1 and hypocretin-2 (HCRT-1 and HCRT-2, respectively) are expressed exclusively in the lateral hypothalamus (1, 2), and *Hcrt* expression shows a diurnal pattern with a peak during the active phase (3). Hcrt signaling is linked to active waking behaviors (4, 5).

Narcolepsy type 1 (NT1) patients have almost no signal from *HCRT* mRNA in the brain and low levels of HCRT-1 in the cerebrospinal fluid (6). Narcolepsy patients suffer from excessive daytime sleepiness and cataplexy (loss of muscle tone triggered by strong emotions), and *Hcrt* knockout animals also experience more sleep episodes during the active phase and cataplexy (7). Optogenetic stimulation of Hcrt neurons during sleep causes transition to wakefulness (8), and overactivity of the Hcrt was suggested as being one of the underlying causes of insomnia (9). Despite its clinical importance, the intracellular regulation of *Hcrt* expression is poorly understood. Some transcription factors, such as FOXA2, NR6A1, and Ebf2, can regulate *HCRT* gene expression, while IGFBP3 acts as a transcriptional regulator (see ref. 10 for a review).

MicroRNAs (miRNAs) are short (20 to 25 nucleotides), noncoding regulatory RNA molecules that exert their effects on target genes by complementary binding of the miRNA strand to the mRNA target sequence, predominantly in the 3′-untranslated region (UTR), leading to either mRNA degradation or translational arrest. Presently, much research is focused on the development of therapeutic miRNAs and delivery systems, and miRNA-based therapeutics are expected to be introduced into the market within the next decades. In parallel with this development, in-depth knowledge on the function of disease-relevant miRNAs is needed.

In vertebrates, more miRNAs are expressed specifically in the brain than in any other tissue (11). Previous studies identified specific miRNAs that regulate neuronal plasticity (12) and circadian rhythms (13, 14), but no specific miRNA was shown to regulate the neurotransmitters or neuropeptides involved in sleep regulation. Here, we investigate miRNAs that could target *HCRT* mRNA. We demonstrate that miRNA-137 (miR-137) regulates *HCRT* expression in vitro and in vivo and that manipulations of miR-137 levels alter the vigilance states in both mice and zebrafish. miR-137 is genetically associated with schizophrenia and involved in the etiology of neuropsychiatric disorders (12, 15–18). Here, we examine whether the *MIR137* locus is also associated with a

Competing interest statement: B.R.K. consults for Union Chimique Belge (UCB) Pharma, Lundbeck, and Orexia Therapeutics unrelated to this work. B.R.K. is a founder of the spin-out company Ceremedy ApS. All other authors declare that they have no competing interests.

This article is a PNAS Direct Submission.

[1]To whom correspondence may be addressed. Email: anjaholmnordvang@gmail.com.

[2]A.H. and M.-L.P. contributed equally to this work.

[3]M.T. and B.R.K. contributed equally to this work.

This article contains supporting information online at http://www.pnas.org/lookup/suppl/doi:10.1073/pnas.2112225119/-/DCSupplemental.

Published April 22, 2022.

range of sleep disorders and phenotypes, and we demonstrate an association with sleep duration.

Results

In Silico Prediction of miRNAs That Target the *HCRT* Neuropeptide Precursor mRNA. We first screened for potential miRNAs that target human *HCRT* using four target prediction algorithms (MicroCosm, TargetScan, DIANA, and PITA) available from "The miRNA body-map" (19). All of these in silico algorithms predicted that hsa-miR-137, hsa-miR-637, and hsa-miR-654-5p target the 3′-UTR of *HCRT* with 7- or 8-mers (Fig. 1 *A* and *B*). Several other poorly conserved miRNAs potentially target *HCRT* but were not predicted by all four algorithms (*SI Appendix*, Fig. S1*A*). Of the predicted human miRNAs, only miR-137 is conserved across species, while among the predicted murine miRNAs, miR-665 was also predicted with moderate confidence to target human *HCRT* (Fig. 1*A* and *SI Appendix*, Fig. S1*A*). Fig. 1*B* shows thermodynamic predictions of the interaction between the miRNAs and the corresponding 3′-UTR of human *HCRT* and mouse *Hcrt*. It has been suggested that G:U wobble base pairing is tolerated as a match for both RNA degradation and translation repression (20). When G:U wobble interactions are included in our analysis, miR-665 interacts strongly with hypocretin in mice and humans (*SI Appendix*, Fig. S1*B*), suggesting that the miRNA:Hcrt interaction is also conserved for miR-665.

To test the functional interaction of the predicted miRNAs with human *HCRT* mRNA in vitro, we wanted to use a cell line with endogenous expression of *HCRT*. We therefore quantified the endogenous expression of *HCRT* mRNA and the miRNAs in 14 human cell lines and found that SK-N-MC and SK-N-DZ neuroblastoma cell lines expressed Hcrt, miR-137, and miR-654, but not miR-637 (*SI Appendix*, Fig. S2). We next investigated the miRNA:Hcrt interaction in SK-N-MC and SK-N-DZ lines by transfecting them with precursor (pre) miRNAs or scrambled pre-miRNAs (scr) as controls. Quantitative real-time PCR (qRT-PCR) analysis confirmed the formation of mature miRNAs in both cell lines (Fig. 1*C* and *SI Appendix*, Fig. S3*A*). We then measured the *HCRT* mRNA levels in both cell lines 24 h after transfection and found that overexpression of miR-137, miR-637, and miR-654-5p suppressed *HCRT*. None of the miRNAs consistently induced expression of any of the other miRNAs tested (Fig. 1*C* and *SI*

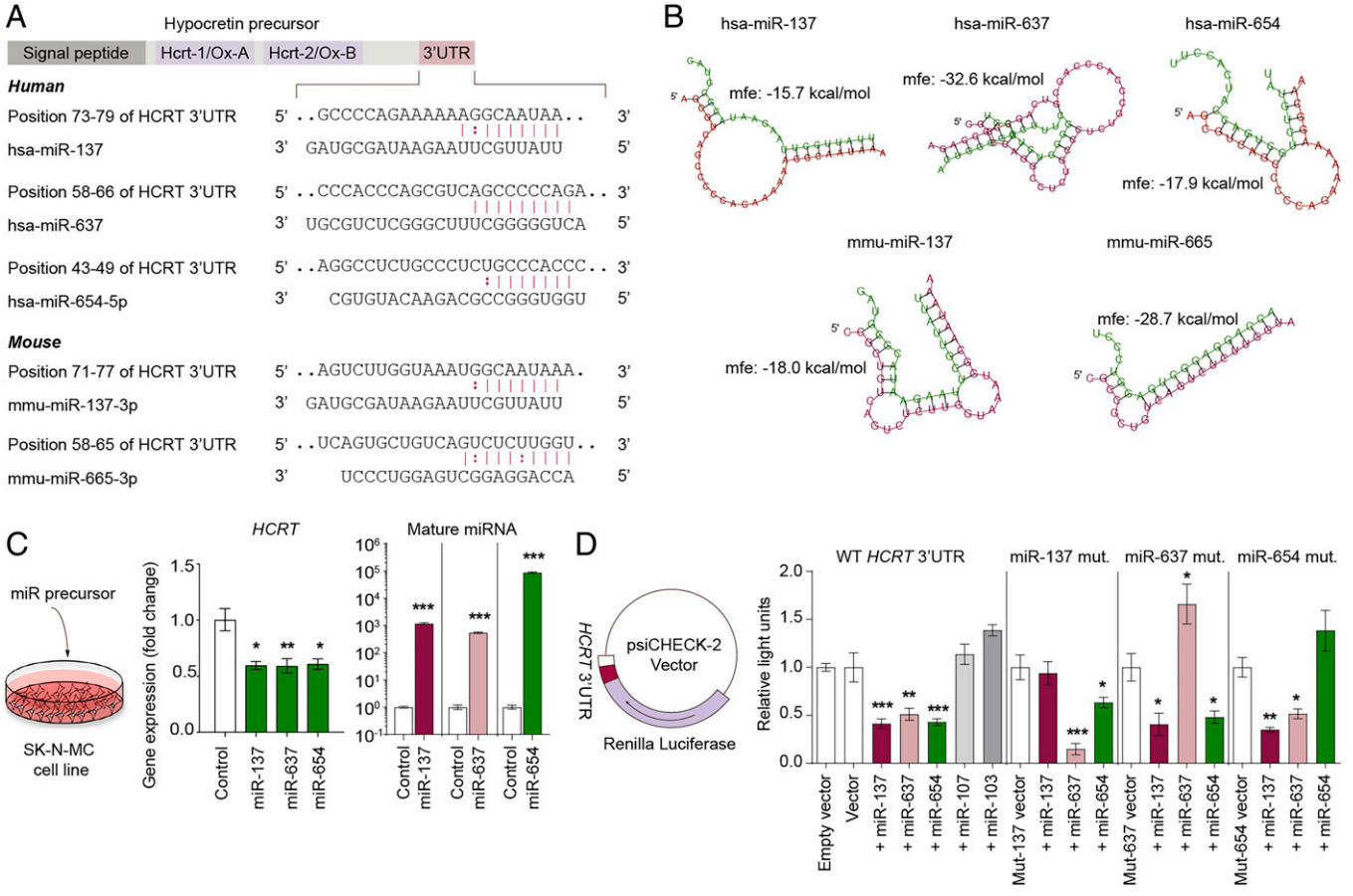

Fig. 1. Identification, characterization, and conservation of miRNAs targeting *HCRT*. (*A*) In silico prediction of *HCRT*-targeting miRNAs (from the miRNA body-map). hsa-miR-137, hsa-miR-637, and hsa-miR-654-5p were predicted to target human *HCRT*. mmu-miR-137-3p and mmu-miR-665-3p were predicted to target *Hcrt* in mice. (*B*) Thermodynamic energy prediction for the association of human *HCRT* 3′-UTR or mouse *Hcrt* 3′-UTR with the predicted miRNAs. Green: miRNAs; red: Human *HCRT*/mouse *Hcrt* sequence. (*C*) Effect on *HCRT* levels following overexpression of precursor hsa-miR-137 ($n = 5$), hsa-miR-637 ($n = 6$), hsa-miR-654-5p ($n = 3$), or scrambled miRNA control ($n = 8$) in the human neuroblastoma cell line SK-N-MC. RNA levels are presented as the magnitude of difference from the control ± SEM; $^{*}P < 0.05$; $^{**}P < 0.01$; one-way ANOVA with Dunnett's post hoc test. The mature miRNA level was quantified in the same cells and are presented as fold change compared to control ± SEM $^{***}P < 0.001$, two-tailed Student's *t* test for each independent experiment as marked with vertical lines. (*D*) Direct miRNA-mediated downregulation of the luciferase signal with the 3′-UTR of *HCRT* cloned into the psicheck-2 luciferase vector. The vector and miRNAs were cotransfected into HEK-293 cells. miR-107 and miR-103 were used as negative controls as these do not target *HCRT*. Mutation of miR-137-seed site:mut-137, mutation of miR-637-seed site:mut-637, and mutation of miR-654-5p-seed site:mut-654. Data were normalized to the control vector in each experiment ± SEM ($n = 5$/condition). $^{*}P < 0.05$; $^{**}P < 0.01$; $^{***}P < 0.001$; four separate one-way ANOVA with Dunnett's post hoc tests are used compared to the control groups vector, Mut-137 vector, Mut-637 vector, or Mut-654 vector. The four experiments are separated by vertical lines.

Appendix, Fig. S3 *B–H*). We confirmed the direct interaction of the miRNAs with the 3′-UTR of *HCRT* using a luciferase reporter assay as well as mutating the miRNA seed sites individually (Fig. 1*D*). Taken together, these results show that miR-137, miR-637, and miR-654-5p regulate *HCRT* expression in vitro.

Proof of Concept That miR-137 and miR-665 Can Regulate *Hcrt* and HCRT-1 Peptide Levels In Vivo. To test whether the miRNAs could also regulate *Hcrt* expression in vivo, we performed intracerebroventricular (ICV) injection of the miRNAs or anti-miRNA oligonucleotides into the brain of mouse pups directly through the skull. For this analysis, we chose the two miRNAs that showed the best predictions in mice, namely, miR-137-3p and miR-665-3p. The low myelin content of the pup brains allows the injected substance to diffuse widely and is a simple model to test whether miRNAs modify the expression of *Hcrt* expression in vivo (21). We first confirmed that, consistent with the findings of previous studies in rat pups (22, 23), *Hcrt* mRNA and peptide were expressed in the brain of postnatal day 1 (P1) to P4 mouse pups (*SI Appendix*, Fig. S4 *A* and *B*). We then performed ICV injection of a mixture of miR-137-3p/miR-665-3p mimics or scrambled controls into P4 mice pups. Trypan Blue was added to confirm the injection site and the widespread diffusion (*SI Appendix*, Fig. S4*C*) (21). Two rounds of injections were performed. Brains from the first round were used for miRNA and mRNA quantifications ($n = 25$), while brains from the second round were used for HCRT-1 peptide quantification ($n = 15$). Compared with controls, we found that miR-137-3p and miR-665-3p levels were significantly higher in the miR-137-3p/665-3p-mimic–treated pups ($P = 0.001$ and 0.002, respectively; $n = 16$ [control] and $n = 9$ [miR-137-3p/665-3p]; two-tailed Student's *t* test, Fig. 2*B*). We further observed a 44% lower level of *Hcrt* expression after miRNA mimic injection compared with controls ($P = 0.035$. $n = 13$ [control] and $n = 9$ [miR-137-3p/665-3p]; Fig. 2*B*). To test the effect of a downregulation of the miRNAs, we performed ICV injections of a mixture of anti-miR-137-3p/anti-miR-665-3p ($n = 15$) or scrambled controls ($n = 7$) into P4 mice pups. This resulted in lower miR-137-3p and miR-665-3p levels in the anti-miR-137-3p/665-3p–treated pups ($P < 0.0001$, $n = 15$ [control] and 7 [anti-miR-137-3p/665-3p]; two-tailed Student's *t* test, Fig. 2*B*). We did not find any effect on *Hcrt* level following anti-miRNA injection; however, we measured the HCRT-1 peptide levels in the same brains and found a 32% lower and a 41% higher level in HCRT-1 peptide expression after miRNA mimic and anti-miRNA treatments, respectively (anti-miRNA vs. control: $P = 0.018$; $n = 15$ (control) and $n = 7$ [anti-miR-137-3p/665-3p], two-tailed Student's *t* test; Fig. 2*B*). As a control, we used the *Pcbd* (Pterin 4 alpha carbinolamine dehydratase) gene, which is colocalized with Hcrt but not targeted by these miRNAs (24), and found that its expression was not affected by the injections (Fig. 2*B*). These results indicate that miR-137-3p and miR-665-3p can regulate both *Hcrt* mRNA and HCRT-1 peptide levels in vivo.

Neuroanatomical Distribution of miR-137 and miR-665 in the Mouse Brain and Expression Level in Mouse Hypothalamus in the Rest and Active Phases. Hsa-miR-137 and mmu-miR-137 are strongly expressed in the brain of humans and mice, respectively (19, 25), whereas miR-665 is not well characterized. To assess the neuroanatomical distribution of the *Hcrt*-targeting miRNAs, we first conducted in situ hybridization in fresh-frozen mouse brain sections, using 5′- and 3′-digoxigenin–labeled locked nucleic acid (LNA) probes targeting mmu-miR-137-3p and mmu-miR-665-3p and found that both miRNAs are widely expressed in the brain, including in the lateral hypothalamus (*SI Appendix*, Fig. S5), consistent with the findings of previous studies (26). We then analyzed if mmu-miR-137-3p and mmu-miR-665-3p colocalize with the HCRT-1 peptide using immunohistochemistry combined with fluorescence in situ hybridization (Fig. 3*A*). Both miRs were present in all HCRT-1–positive neurons observed.

We next investigated the endogenous expression levels of miR-137-3p and miR-665-3p in the hypothalamus at different time points. We previously reported the diurnal variation of *Hcrt* mRNA and HCRT-1 peptide in the mouse brain (3). Using the same brain samples, we quantified miR-137-3p and miR-665-3p expression in four groups of mice, which were euthanized at different time points over 24 h, and found a clear difference in their expression over time, with the highest levels of both miRs at zeitgeber time interval 18 to 24 (ZT18-24) (miR-137-3p ZT0-6 vs. ZT18-24, $P = 0.012$; miR-137-3p ZT6-12 vs. ZT12-18, $P = 0.016$; miR-137-3p ZT12-18 vs. ZT18-24, $P = 0.0002$; miR-665-3p ZT0-6 vs. ZT18-24, $P = 0.011$; miR-665-3p ZT12-18 vs. ZT18-24, $P = 0.0001$; Hcrt ZT0-6 vs. ZT18-24, $P = 0.0015$; Hcrt ZT6-12 vs. ZT18-24, $P = 0.0004$; nonparametric Kruskal-Wallis test followed by Dunn's multiple comparisons; Fig. 3*B*). Overall, the total level of miR-137 was much higher than miR-665 based on their relative differences (Fig. 3*C*). It was demonstrated before that the endogenous miR-137 level is high in the brain (27, 28). These data show that miR-137-3p and miR-665-3p are expressed in Hcrt neurons and their expression varies significantly over the course of 24 h. This is in concordance with our hypothesis that miR-137-3p and miR-665-3p are involved in the regulation of *Hcrt* expression in mice.

Specific Inhibition of miR-137 in Hcrt Neurons Increases Wakefulness. We demonstrated that miR-137 is highly expressed in the hypothalamus, is present in Hcrt neurons, and has the capacity to regulate *Hcrt* levels. Since the levels are high, we asked whether miR-137 under normal circumstances is partially blocking *Hcrt* expression. This means that the downregulation of miR-137 we observe at ZT12-18 could be functionally important for allowing *Hcrt* expression to increase to stabilize wakefulness in the same time interval. To investigate the hypothesis that miR-137 downregulation will cause an increase in *Hcrt*, we injected viral vectors containing a sponge sequence of these miRNAs into the lateral hypothalamus of Hcrt-Cre mice (Fig. 4*A*). We also included an miR-665 sponge and an unrelated miR-128 sponge as a control in the experiment. With this method, the miRs are inhibited by binding to the sponge, specifically in Hcrt neurons. Our results indicated a resulting 3.7-fold and 2.5-fold higher levels of *Hcrt* expression, with inhibition of miR-137 and miR-665, respectively. The upregulation following miR-137 inhibition was statistically significant ($P = 0.039$, one-way ANOVA; Dunnett's post hoc test, $n = 5$ for anti-miR-137, $n = 6$ for anti-miR-665, and $n = 5$ for control; Fig. 4*B*). We also quantified the amounts of wakefulness and non-rapid eye movement (NREM) sleep at 4-h intervals over 24 h in a subset of these mice (Fig. 4*C*). We found that Hcrt neuron-specific inhibition of miR-137 was associated with significantly more wakefulness than in control mice, during the first 4 h of the dark period (ZT12-16). There was 24 ± 10% more wakefulness in anti-miR-137-injected animals than in controls during this period (anti-miR-137–injected vs. control: $P = 0.037$; one-way ANOVA with Dunnett's post hoc test, $n = 5$ for miR-137, $n = 7$ for control;

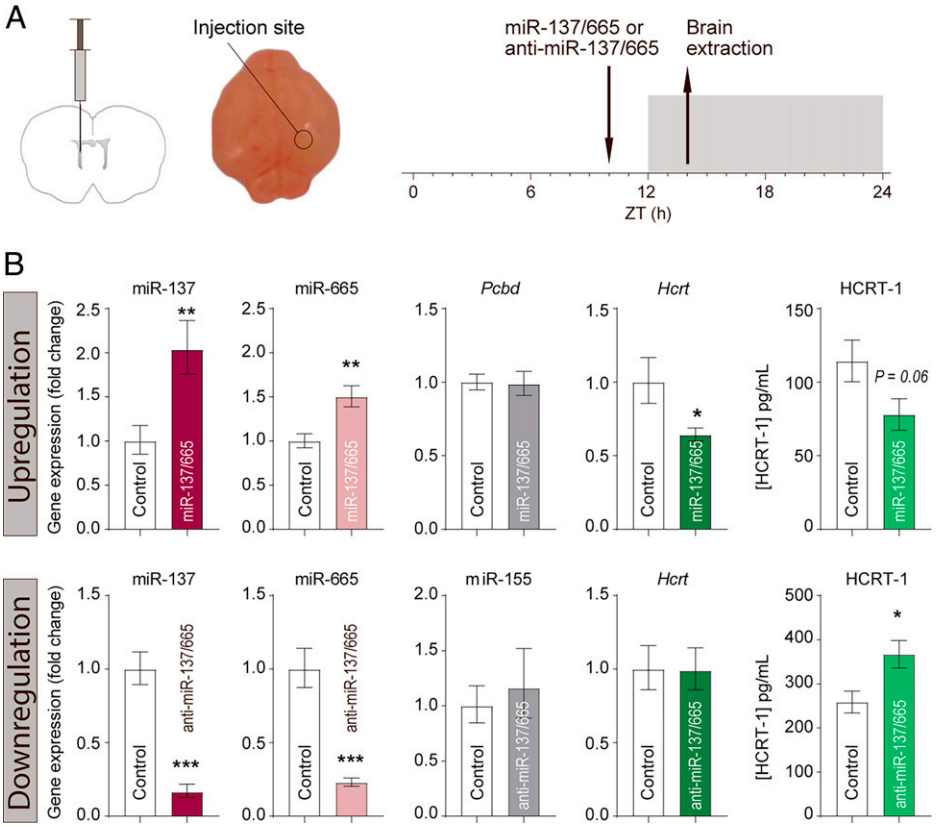

Fig. 2. In vivo targeting of *Hcrt* by miR-137-3p and miR-665-3p. (*A*) Schematic representation of ICV injection in P4 mouse pups. (*B*) Injection of a mixture of mmu-miR-137-3p/miR-665-3p mimics ($n = 9$) and anti-miR-137-3p/anti-miR-665-3p ($n = 7$) in P4 pups. Littermate controls were injected with a scramble ($n = 16$ per group) or an antiscramble ($n = 15$). RNA was isolated and analyzed by qRT-PCR. Data are presented as the magnitude of the difference compared with controls ± SEM. HCRT-1 peptide was extracted from the brains and analyzed by radioimmunoassay (RIA) (upregulation by miRNA mimic, $n = 8$ vs. controls $n = 7$; downregulation by anti-miR, $n = 15$ vs. controls $n = 7$). Counts are normalized to control and presented as mean ± SEM. *Pcbd*: Pterin-4-alpha-carbinolamine dehydratase function as the control since it is not a target of mmu-miR-137-3p/miR-665-3p. miR-155 is included as a control to illustrate that miRNAs in general are not affected by anti-miR injections. $^*P < 0.05$; $^{**}P < 0\ 0.01$; $^{***}P < 0.001$, two-tailed Student's *t* test.

Fig. 4*C*). Accordingly, we found significantly less NREM sleep in anti-miR-137 animals compared with controls during the same 4 h of the dark period (Fig. 4*D*). There was 56 ± 22% less NREM sleep in anti-miR-137 animals than in controls (anti-miR-137–injected vs. control: $P = 0.031$; one-way ANOVA with Dunnett's post hoc test; $n = 5$ for anti-miR-137, $n = 7$ for control; Fig. 4*D*). No significant differences were found between anti-miR-665–injected and control mice for wakefulness or NREM sleep. These results indicate that inhibition of miR-137 consolidates wakefulness during the early hours of the dark period, which is consistent with the circadian time when endogenous *Hcrt* mRNA expression starts to increase (Fig. 3*B*).

To investigate whether the greater wakefulness in anti-miR-137-injected animals results from longer wakefulness episodes or simply from more episodes, we quantified the distribution of bout durations (Fig. 4*E*). We found that anti-miR-137 animals had significantly fewer short wakefulness episodes and more long wakefulness bouts compared with the control group (anti-miR-137 vs. control: $P = 0.004$ for 4- to 8-s episodes, $P = 0.014$ for >512-s episodes; two-way ANOVA with Dunnett's post hoc test). No significant differences were found in the distribution of bout durations between anti-miR-665 animals and controls. We further assessed the dynamics of delta power (0.75 to 4 Hz) during NREM sleep, as a marker of sleep intensity (29, 30), and found a tendency toward higher values (23 ± 8%) in anti-miR-137-injected animals compared to controls during the dark period (Fig. 4*F*, $P = 0.063$; one-way ANOVA with Dunnett's post hoc test). These results indicate that the inhibition of miR-137 in Hcrt neurons leads to increased *Hcrt* levels and increased wakefulness as a result of longer wake episodes.

Overexpression of miR-137 or miR-665 Cause a Downregulation of *Hcrt* Expression That Is Compensated over Time. We next aimed to test the effect of miR-137-3p and miR-665-3p overexpression specifically in Hcrt neurons. To this end, we designed recombinant adeno-associated virus (rAAV) vectors containing the mature miRNA sequence driven by the murine *Hcrt* promoter (*SI Appendix*, Fig. S6*A*) (8), delivered by stereotaxic microinjection into the lateral hypothalamus of adult mice. Three different rAAV vectors were used carrying miR-137-3p, miR-665-3p, or a nonsilencing scrambled miRNA control. Seven days following rAAV vector injections, we found a significant downregulation of *Hcrt* mRNA ($P = 0.036$, one-way ANOVA with Dunnett's post hoc test comparing treatment to control, $n = 6$ for anti-miR-137, $n = 6$ for anti-miR-665, and $n = 5$ for control; *SI Appendix*, Fig. S6*B*). It was not possible to measure the miR levels only in the Hcrt neurons, so we quantified the miRs in whole hypothalamus homogenate. Here, we could not detect an increase in miR levels (*SI Appendix*, Fig. S6*B*). This is not surprising as both miRs are expressed in many other cell types in the area, and furthermore, the Hcrt neurons are only a small fraction of all hypothalamic cell types. With time, there appeared to be a compensatory upregulation of *Hcrt* expression (*SI Appendix*, Fig. S6*C*). Despite this compensatory

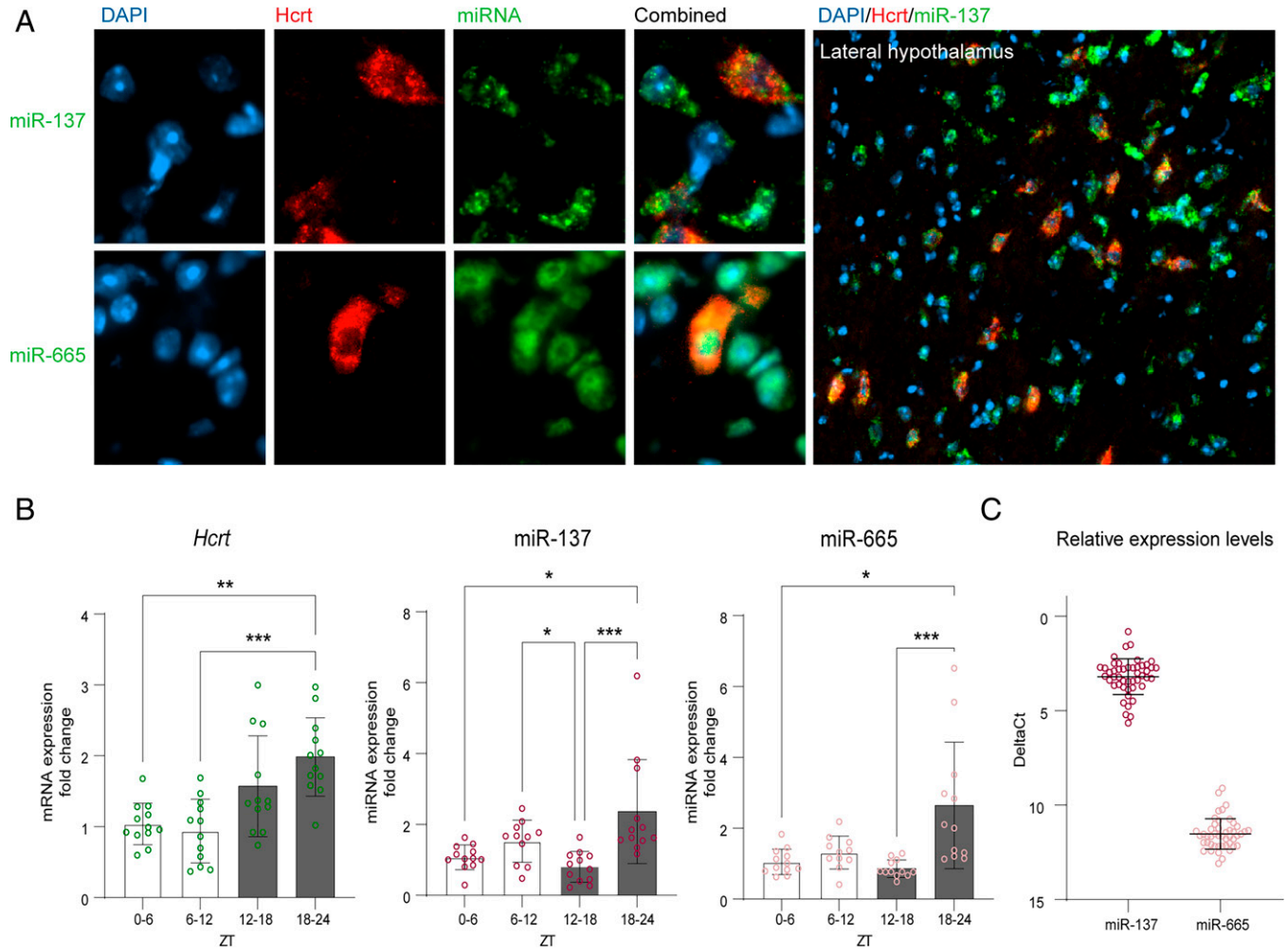

Fig. 3. Correlation between hypocretin expression and miRNA diurnal variations. (*A*) Single neurons from mouse brain sections that were immunostained with HCRT-specific antibody (red) following in situ hybridization with LNA-mmu-miR-137-3p or LNA-mmu-miR-665-3p-specific probes (green). *Upper Right* shows colocalization of mmu-miR-137-3p with Hcrt-positive cells in the lateral hypothalamus of the mouse brain. All detected Hcrt neurons coexpressed miR-137. (*B*) Expression of miR-137, miR-665, and *Hcrt* mRNA in the mouse hypothalamus at different zeitgeber time intervals (ZTs). The gray bars represent the dark phase; n = 12/group animals at each time interval. Data were analyzed with the nonparametric Kruskal–Wallis test followed by Dunn's multiple comparisons of all time points compared to all other time points $^{*}P < 0.05$; $^{**}P < 0.01$; $^{***}P < 0.001$. (*C*) Relative expression levels of miR-137 and miR-665 in the hypothalamus. DeltaCt is the difference between the level of two endogenous control genes U6 and SNO202 as measured by qRT-PCR and the miR level. High deltaCt equals a low expression level, and therefore, we depict the y axis in reverse. n = 48/group.

effect, we still detected a significant 20.4% decrease in caudal HCRT-1 levels after miR-665 upregulation ($P = 0.024$, one-way ANOVA with Dunnett's post hoc test comparing treatment to control, $n = 8$ for anti-miR-137, $n = 9$ for anti-miR-665, and $n = 8$ for control; *SI Appendix*, Fig. S6*D*). It was previously shown that HCRT protein needs to be more than ∼85% downregulated to see functional effects (31). It is thus unlikely that the effects that we observe after upregulation of miR-137 or miR-665 cause substantial functional changes. These data demonstrate that overexpression of miR-137 and miR-655 can lead to changes in the ratio of *Hcrt* mRNA to peptide, but we also show that the overexpression led to a compensatory response with time.

IL-13 Upregulates miR-137 and Downregulates *Hcrt* Expression. It could be argued that massive overexpression of the miRNAs is very artificial, so to test a more physiological relevant upregulation of the miRNA, we decided to test the effect of various cytokines. Previous studies described the role of different cytokines, e.g., tumor necrosis factor alpha (TNF-α), interferon beta (IFN-β), interferon gamma (IFN-γ), and interleukin-13 (IL-13), in regulating *Hcrt* expression (24, 32–34). We therefore tested whether the regulation of *Hcrt* expression by any of these cytokines could be due to an upregulation of miR-137. To this end, we stimulated the human cell line SK-N-DZ with TNF-α, IFN-β, IFN-γ, and IL-13 and found that among these, IL-13 showed a dose-dependent significant upregulation of miR-137 expression while also downregulating *Hcrt* (one-way ANOVA: $F(3, 53) = 4.822$, $P = 0.0048$; Dunnett's post hoc test: $^{**}P = 0.0085$ IL-13 0.01 μg/mL vs. control , $^{**}P = 0.0075$ IL13 0.05 μg/mL vs. control; Fig. 5*A*). Results from the other cytokines are shown in *SI Appendix*, Fig. S7. IL-13 receptor expression was reported to be 17-fold higher in Hcrt neurons compared to other neurons (24), and IL-13 might therefore target Hcrt neurons more specifically than other cytokines. Thus, we tested the effects of IL-13 treatment in vivo when injected at ZT10 before the dark-to-light transition (Fig. 5*B*). Our data show that the expression of miR-137-3p and miR-665-3p increased at ZT18 in IL-13–injected mice (both $n = 11$) compared with controls ($n = 10$ and 9, respectively. $^{*}P = 0.0111$ and 0.0177, respectively; two-way ANOVA with Sidak post hoc comparisons of treatment vs. control groups. Fig. 5*C*). As hypothesized, *Hcrt* mRNA expression was significantly downregulated in the same brains ($^{*}P = 0.0340$, two-

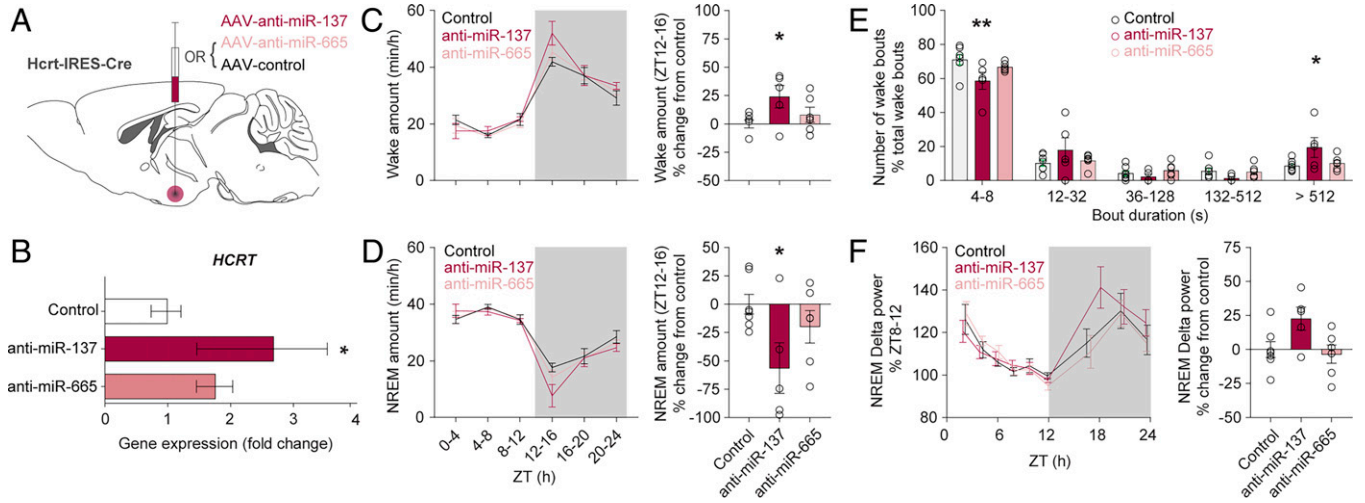

Fig. 4. Targeted downregulation of miR-137 in Hcrt neurons consolidates wakefulness. (*A*) Schematic representation of local injection of AAVs in the lateral hypothalamus of Hcrt:IRES-Cre driver mice. (*B*) Expression levels of *Hcrt* in murine brain after rAAV-anti-miR-137, rAAV-anti-miR-665, and rAAV-anti-miR-128 overexpression, specifically in the Hcrt-producing neurons. rAAV-anti-miR-128 was used as a control, as it does not target *Hcrt*. Mice were euthanized at 5 wk postinjection. Differences between the anti-miR and control groups were analyzed using a one-way ANOVA with Dunnett's post hoc test. $*P = 0.039$. (*n*: control = 5; anti-miR-137 = 5; anti-miR-665 = 6 animals). (*C* and *D*) Quantification of vigilance states per 4-h intervals over 24 h. Local expression of anti-miR-137 in Hcrt neurons increases wakefulness (*C*) and accordingly decreases NREM sleep (*D*), compared with control mice during the first 4 h of the dark period (ZT12-16). There is a significant increase of 24.1 ± 9.9% in the duration of wakefulness and a reduction of 56.4 ± 22.3% in that of NREM sleep, in anti-miR-137-injected animals during ZT12-16 (anti-miR-137 vs. control: $*P < 0.05$ for wakefulness and NREM; anti-miR-665 vs. control: $P > 0.05$ for wakefulness and NREM; one-way ANOVA with Dunnett's post hoc test. *n*: control = 7; anti-miR-137 = 5; anti-miR-665 = 6 animals). (*E*) Distribution of wakefulness bout durations shows significantly longer bouts in anti-miR-137–injected animals compared with controls during ZT12-16 (anti-miR-137 vs. control: $**P < 0.01$ for 4- to 8-s bouts of wakefulness; $*P < 0.05$ for >512-s bouts; two-way ANOVA with Dunnett's post hoc test. *n:* control = 7; anti-miR-137 = 5; anti-miR-665 = 6 animals). (*F*) Dynamics of NREM delta (0.75 to 4 Hz) power over 24 h indicates a tendency that anti-miR-137–injected animals have higher EEG delta power (22.8 ± 8.5) in the first percentile of NREM sleep during the dark period compared with controls (anti-miR-137 vs. control: $P = 0.063$; anti-miR-665 vs. control: $P > 0.05$; one-way ANOVA with Dunnett's post hoc test. *n*: control = 7; anti-miR-137 = 5; anti-miR-665 = 6 animals).

way ANOVA with Sidak post hoc comparisons of treatment vs. control groups; $n = 11$ IL-13 mice, $n = 10$ control mice; Fig. 5*D*). IL-13 injection did not significantly change the expression of miR-137-3p, miR-665-3p, and *Hcrt* at ZT14 and ZT24 or HCRT-1 levels (Fig. 5 *C* and *D*). These results suggest that IL-13 might downregulate *Hcrt* mRNA by upregulating miR-137-3p and miR-665-3p expression in human neuroblastoma cells and in the mouse hypothalamus.

Inhibition of miR-137 in Zebrafish Reduces Sleep and Increases Locomotor Activity. miR-137 is highly conserved across species from fish to humans (35). To investigate the effects of its inhibition in zebrafish, *Danio rerio*, we injected an anti-miR-137 morpholino (Mo-miR-137) into zebrafish embryos and quantified their activity and sleep/wake cycle. To avoid developmental and morphological abnormalities, a low concentration of 8 ng Mo-miR-137 was injected, as suggested in previous studies (35). To assess the impact of miR-137 inhibition on the sleep/wake distribution, we continuously recorded zebrafish locomotion for 3 d, from 5 to 8 d postfertilization (dpf), as previously described (36, 37). Larvae with morphological defects were excluded in both groups (8.9 ± 1.2% Mo-miR and 1.5± 0.7% Mo-control) to limit a potential extraneous bias due to the morphological defect and locomotion impairment (Fig. 6*A*). Inhibition of miR-137 significantly increased activity during the light period compared with control fish injected with a commonly used control morpholino (Mo-miR-137 vs. Mo-control: $P = 0.043$ for light 5 dpf, $P = 0.0013$ for light 6 dpf, $P < 0.001$ for light 7 dpf; two-way ANOVA with Sidak post hoc test, degrees of freedom [DF] = 5, F (5,470) = 13.76; $n = 48$ fish per group; Fig. 6*B*). Accordingly, Mo-miR-137-injected fish had significantly less sleep during all three dark periods, as well as during the third light period, compared with Mo-controls (Mo-miR-137 vs. Mo-control: $P < 0.001$ for dark 5 to 7 dpf, $P = 0.0073$ for light 7 dpf; two-way ANOVA with Sidak post hoc test; DF = 5, F (5,470) = 2.79; $n = 48$ fish per group; Fig. 6*C*). These results show that miR-137 plays a role in sleep regulation also in zebrafish. There are possible target sites for miR-137 in zebrafish *hcrt* mRNA (*SI Appendix*, Fig. S8), but since we performed a global manipulation, the effect is likely mediated via many different miR-137 targets. Overall, our findings in zebrafish support what we find in mice and suggest a conserved role for miR-137 in regulating sleep and wakefulness.

The Human miR-137 Gene Is Associated with Sleep Duration. To investigate whether miR-137 is also involved in regulating human sleep, we analyzed data from a genome-wide association study (GWAS) of 19 different sleep-related phenotypes included in the UK Biobank. A strong association was seen between single-nucleotide polymorphisms (SNPs) in the *MIR137* locus (chr1: 98453556 to 98515419 (GRCh37/hg19)) and sleep duration but not with any of the other phenotypes. GWASs carried out to date using sleep duration data from the UK Biobank have identified the nearby gene *DPYD* (38–40), which encodes dihydropyrimidine dehydrogenase, an enzyme involved in the breakdown of pyrimidines. *DPYD* is not yet functionally linked to sleep regulation, and our data suggest that *MIR137* might instead be the functionally relevant target gene in the locus. Indeed, the lead SNP rs12567114 is located in close proximity (12,532 bp upstream) to the *MIR137* gene (Fig. 7). This shows that human sleep duration is genetically associated with the *MIR137* locus and suggests that individual differences in sleep duration could be partly determined by its effects on miR-137 expression.

Discussion

Here, we describe a mechanism by which miRNAs regulate expression of the wake-promoting HCRT peptides. By combining *in silico* prediction with in vitro and in vivo experiments,

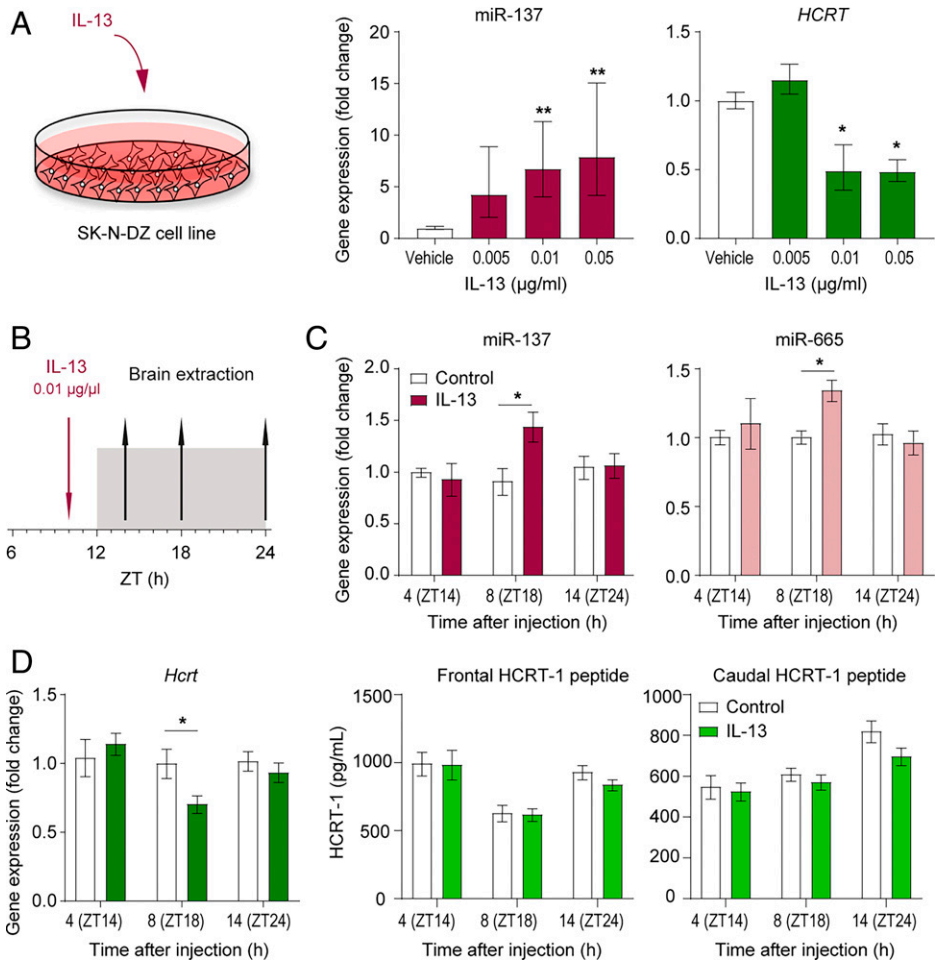

Fig. 5. IL-13 induces miR-137 upregulation and *HCRT* downregulation in vitro and in vivo. (*A*) Stimulation of human neuroblastoma cells (SK-N-DZ) with IL-13 at concentrations of 0.005 ng/μL (n = 9), 0.01 ng/μL (n = 15), and 0.05 ng/μL (n = 12). RNA was isolated and miR-137 and *HCRT* expression analyzed by qRT-PCR. Data are from seven independent cell culture experiments and presented as the mean fold change difference compared with vehicle ± SEM (one-way ANOVA with Dunnett's post hoc test comparing to vehicle group; *P < 0.05; **P < 0.01). (*B*) Schematic overview of IL-13 injection (0.01 μg/μL, intraperitoneal) and timing of termination. (*C*) Expression analysis of mmu-miR-137 (ZT18 control vs. IL-13 injection; n = 10 and 11, respectively) and mmu-miR-665 (ZT18 control vs. IL-13 injection; n = 9 and 11, respectively). Data are presented as the magnitude of difference compared with vehicle ± SEM (two-way ANOVA with Sidak post hoc comparisons of treatment group to control group at each time point; *P < 0.05). (*D*) *HCRT* mRNA determined by qRT-PCR and HCRT-1 peptide levels determined by RIA. ZT18 control vs. IL-13 injection; n = 10 and n = 11, respectively. Data are presented as mean ± SEM (two-way ANOVA with Sidak post hoc comparisons of treatment group to control group at each time point; *P < 0.05).

we identified miR-137 as an evolutionarily conserved regulator of *Hcrt* expression. Our results suggest that miR-665 could play a similar role. We show that miR-137 and miR-665 are expressed endogenously in Hcrt neurons and that their expression in the hypothalamus varies with the time of day. Most strikingly, we show that downregulation of miR-137 in Hcrt neurons increases *Hcrt* mRNA levels and subsequently strengthens wakefulness at the beginning of the dark period. Using acute injections of miR-137 and miR-665 mimics and viral vector-mediated overexpression, we also show that overexpression of these miRNA can downregulate *Hcrt* but with less impact. Endogenous miR-137 levels in the hypothalamus are high, suggesting that *Hcrt* mRNA might always be partially regulated by miR-137. The lowest levels of miR-137 are seen in the beginning of the dark period coinciding with maximal wakefulness in mice.

miR-137 is one of the most abundant and enriched miRNAs in the brain of adult mice and humans, with a high level of expression in the neocortex and hippocampus and a low level in the cerebellum and brainstem (27, 28). Embryonic development depends on the expression of at least one functional allele of *MIR137*, with embryonic lethality occurring in all homozygous ($^{-/-}$) embryos (41). Clear developmental effects were ascribed to miR-137 (42), but the effects on *Hcrt* expression and wakefulness reported here cannot be explained by such processes, as our manipulations, in vitro and in vivo, were either acute or induced in fully mature adult animals. Importantly, the types of manipulations we performed only partially inhibited the miRNAs and can thus not be compared to full knockout models.

miR-137 is an evolutionarily conserved miRNA. Here, we show that the role of miR-137 in regulating the wake to sleep ratio is present in both mice and zebrafish. This could be ascribed to the interaction between miR-137 and *Hcrt* but could also be due to many other genes targeted by miR-137. It is well known that miRNAs regulate a large number of genes, as is also the case for miR-137 (43). *PDE10A*, *BDNF*, and *CACNA1C* are other known targets of miR-137 (44). The human miR-137 host gene (*MIR137*) has several common variants located within or near the gene on chromosome 1. Here, we used data from the UK Biobank to show that the *MIR137* locus is also associated with sleep duration in healthy individuals. While we clearly demonstrate that miR-137 and its alignment with the *Hcrt* sequence is conserved across mice and

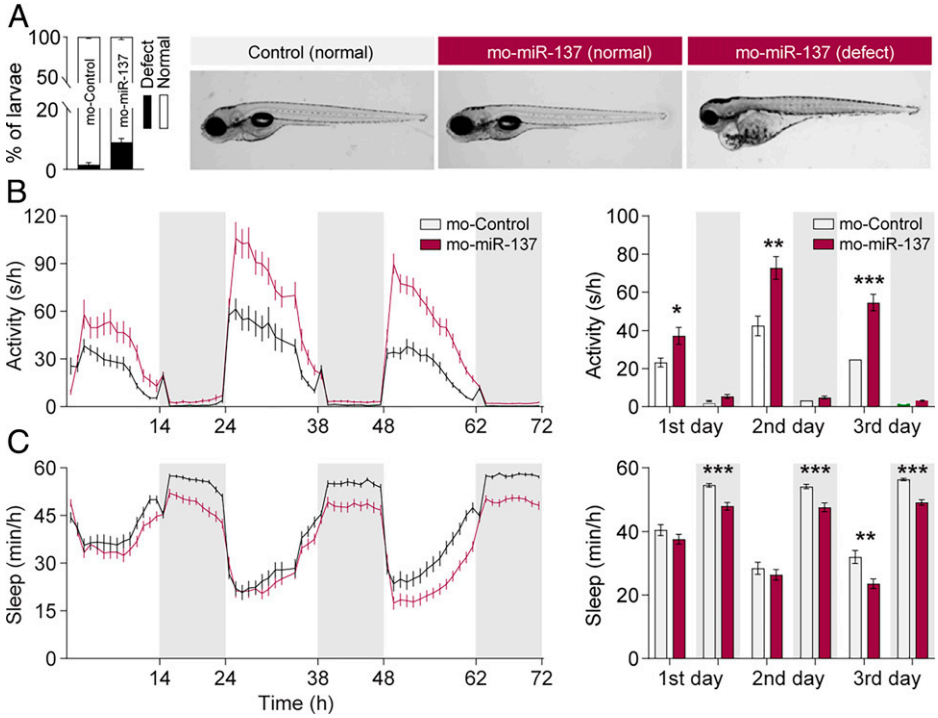

Fig. 6. Knockdown of miR-137 increases locomotor activity and reduces sleep in zebrafish. (*A*) Morphological evaluation of zebrafish after knocking down miR-137. The developmental deficit rate in 5-dpf larvae is less than 10% (*Left*, combined dataset from four independent experiments, Mo-miR-137: $n = 223$, Mo-control; $n = 207$ fish). *Right* shows representative morphological images of normal and abnormal fish (*Right*). (*B*) Time course of the locomotion activity 5 to 7 dpf (*Right*), and the average activity per 14 h:10 h light:dark cycle (*Left*). Mo-miR-137 fish are significantly more active during the light phase than Mo-controls (Mo-miR-137 vs. Mo-control: $P < 0.05$ for light 5 dpf; $P < 0.01$ for light 6 dpf; $P < 0.001$ for light 7 dpf; F = 13.76; DF = 5; two-way ANOVA with Sidak post hoc test; $*P < 0.05$; $**P < 0.01$; $***P < 0.001$; representative figure with Mo-miR-137: $n = 48$, Mo-control; $n = 48$ fish). (*C*) Time course of the amount of sleep 5 to 7 dpf (*Right*), and the average amount of sleep per light/dark cycle (*Left*). Mo-miR-137 fish sleep significantly less during dark periods than Mo-controls (Mo-miR-137 vs. Mo-control: $P < 0.001$ for dark 5 to 7 dpf; $P < 0.01$ for light 7 dpf; F = 2.79; DF = 5; two-way ANOVA with Sidak post hoc test; representative figure with Mo-miR-137: $n = 48$, Mo-control: $n = 48$ fish).

human, our functional zebrafish data and human genetic data offer only circumstantial evidence that there could also be a conserved functional role of the miR-137:Hcrt interaction. More research is needed before firm conclusions can be made.

Our data suggest that miR-137 binding to and inhibiting translation of *Hcrt* mRNA play a posttranscriptional role in *Hcrt* regulation. It would be interesting to know under which physiological circumstances this regulatory mechanism comes into play. Many immune mediators, such as cytokines, have known effects on sleep (45), and several studies reported a direct effect of cytokines on Hcrt neurons (24, 32–34). The mechanisms behind these effects are largely unknown. We therefore tested whether miR-137 and miR-665 could play a role in the regulation of *Hcrt* by cytokines. Our results support the hypothesis that IL-13 regulates the expression of *Hcrt* through changes in miRNA levels. Previous studies also showed that miRNAs are involved in IL-13 signaling in macrophages (46) and fibroblasts (47). We also tested TNF-α, IFN-γ, and IFN-β in vitro, but we found no clear evidence of any effects. As these cytokines have a wide range of functions in the brain, their specific effects on miRNA and *Hcrt* levels might be difficult to detect. Thus, it remains unclear whether the link between IL-13, miR-137, and *Hcrt* is unique. IL-13 could be a more specific regulator of *Hcrt* compared to other cytokines, as its receptor transcript is highly enriched in Hcrt neurons compared to other neurons (24).

Our study shows that noncoding RNAs regulate a neurotransmitter/peptide system involved in homeostatic regulation of the sleep-wake cycle, and our findings raise the question of whether dysregulation of miR-137 is the basis of disturbed sleep under certain circumstances.

Narcolepsy is the model disease of the hypocretin system. In NT1, patients lack hypocretin, and as a result, they suffer from excessive daytime sleepiness and cataplexy, among other sleep-related symptoms (48). The disease is likely to be caused by an autoimmune pathogenesis, even though this is not convincingly proven yet (49). The miRs we describe here are unlikely to play a major role in narcolepsy, as they most likely cannot induce such a massive lowering of HCRT-1 levels as is normally seen in NT1. Even with viral vector-mediated overexpression of the miRs, we only see up to a 20% decrease in Hcrt-1 levels. Interestingly, there are rare instances of narcolepsy with intermediate HCRT-1 levels (50). In these cases, the etiology is completely unknown, and here, one could speculate whether miR-137 is involved. miR-137 could also be involved in insomnia, where too much Hcrt signaling could play a role, or in psychiatric diseases, where sleep is often disturbed. The *MIR137* locus has a strong genetic association with schizophrenia and has also been suggested to be involved in the etiology of other neuropsychiatric disorders (12, 15–18). miR-137 expression is dysregulated in schizophrenia and Rett-syndrome (51–53). Furthermore, microdeletions encompassing *MIR137* are linked to autism and intellectual disability (28, 54). Patients suffering from neuropsychiatric disorders often have poor sleep quality (55, 56). The interaction reported here between miR-137, *Hcrt*, and sleep regulation could therefore play an important role in several neurological and neuropsychiatric diseases featuring disturbed sleep-wake patterns and could pave the way for treatments.

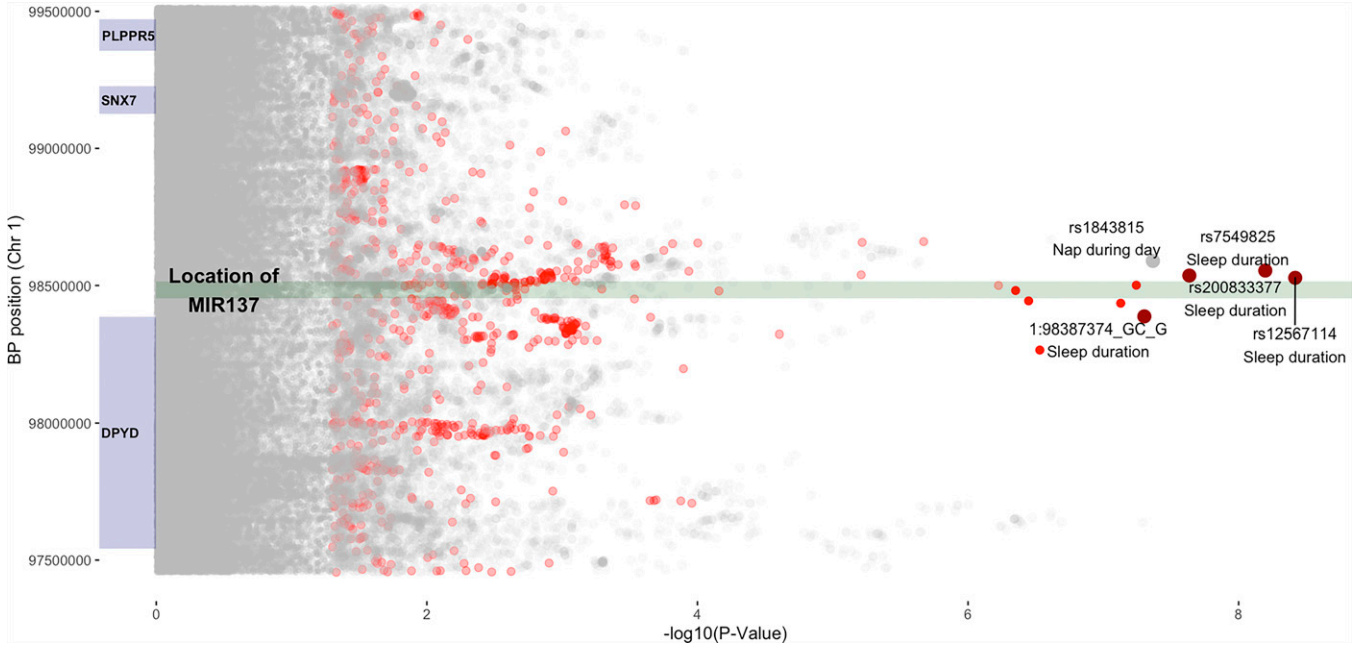

Fig. 7. Genetic associations between sleep duration and the human *MIR137* locus. Chromosome location of *MIR137* with surrounding SNPs and genes. The plot depicts the location of *MIR137* (dark-green box) on chromosome 1 (98453556 to 98515419 GRCh37/hg19). Genes in close genomic proximity (±1,000,000 base pairs) are marked with dark-blue boxes. The $-\log_{10}$-transformed values of *P* values for SNPs of 19 sleep phenotypes from the UK Biobank are plotted on the x axis. All genome-wide-significant SNPs with values of $P \leq$ 5E-8 are marked in dark red and annotated, whereas SNPs from the sleep duration GWAS with a *P* value between 5E-8 and 0.05 are indicated in light red. All other SNPs for different GWAS phenotypes are marked in gray. The size of the points increases with the significance of the SNP association.

Materials and Methods

Cell Culture Experiments. miRNA mimics designed to function as mature endogenous miRNAs were obtained from Thermo Scientific (all miRNA mimics are listed in *SI Appendix*) and transfected using Lipofectamine 2000 into SK-N-MC and SK-N-DZ cells. For the Luciferase reporter assay the 3′-UTR-hypocretin sequence with normal or mutated miRNA seed sites were cloned into the SiCHECK-2 vector (Promega), generating Luciferase reporter constructs. Primers used for cloning and site-directed mutagenesis are can be found in Dataset S1.

Animals. C57BL/6 mice for cytokine injection (only males) and breeding were obtained from Taconic Europe and housed at Glostrup Research Institute (license #2014-15-0204-00008, license #2014-15-0201-00176)). Animals were maintained under standard conditions with constant room temperature (24 °C) and a 12-h light/dark cycle (lights on at 7:00 AM). Standard laboratory food (Altromin 1310) and water were provided ad libitum. P4 mouse pups bred in-house were used for all in vivo ICV injections (license #2014-15-2934-01069).

C57BL/6 mice for AAV injections were obtained from Charles River, and Hcrt-Cre-KI mice were bread locally. Animals were maintained under standard conditions at constant room temperature (22 °C) and a 12-h light/dark cycle (lights on at 7:00 AM). Standard laboratory food and water were provided ad libitum. AAV and electroencephalography (EEG) experiments were carried out in accordance with the BE 113/13 animal regulations and the regulations of the Swiss Federal and State of Vaud Veterinary Offices.

Viral Vector-Mediated miRNA Inhibition and Overexpression. For the development of sponge constructs for inhibiting the miRNAs, recombinant AAV5 miRNA vectors were obtained from Vector Biolabs. The human synapsin 1 gene promoter was used as a specific neuronal promoter. Complementary sequences of the miRNAs were inserted between two lox sites, followed by a GFP marker, to obtain final vectors of pAAV-hSyn-double-floxed EGFP-miR-137-3p-sp for miR-137, pAAV-hSyn-double-floxed EGFP-mir-665-3p-sp for miR-665, and pAAV-hSyn-double-floxed EGFP-miR-128sp for miR-128.

For miRNA overexpression, the following miRNA-AAV vectors were used: mmu-miR-137-3p (stock-keeping unit [SKU]#: AAV-MI0000163), mmu-miR-665-3p (SKU#: AAV-MI0004171), and a control-miRNA vector (mmu-miR-155 scrambled sequence). Serotypes AAV2 and AAV5 were used as inverted terminal repeat and capsid virus, and the EF1a promoter was exchanged with the mouse *Hcrt* promotor.

EEG/Electromyography (EMG) Recordings of Sleep States. For the anti-miRNA study, viral injections in the lateral hypothalamus (anterior-posterior [AP]: −1.4 mm; medial-lateral [ML]: ±1 mm; dorsal-ventral: −5.4 mm) and electrode implantations were performed on mice aged 10 to 12 wk. Animals were anesthetized and fixed in the stereotaxic frame for viral injections and EEG/EMG instrumentation. EEG/EMG electrodes were implanted through the skull in the frontal (AP: +1.5 mm, ML: −1.7 mm to bregma) and the parietal (1.5 mm anterior to lambda, ML: 1.7 mm to bregma) cortices of the right hemisphere and served as EEG electrodes. Two gold wires were placed in the neck muscle to serve as the EMG electrodes. Vigilance states (wake, NREM, and rapid eye movement [REM] sleep) were scored manually in 4-s epochs by visual inspection of concurrent EEG/EMG/video recordings. Power spectral density of EEG recordings was estimated using the discrete Fourier transform of 4-s epochs with a Hanning window and 0.25-Hz frequency resolution.

Inhibition of miR-137 in Zebrafish. Morpholino oligonucleotides were obtained from Gene Tools and injected into 1- to 2-cell zebrafish zygotes (*Danio rerio*; Oregon AB using a microinjector [Femtojet 4i, Eppendorf]). Morpholino sequences were designed according to Giacomotto et al. (35), namely, Mo-Control: 5′-CCTCTTACCTCAGTTACAATTTATA-3′ (human hemoglobin subunit beta gene) and Mo-miR-137: 5′-TTCTTAAGCAATAACAACGAGAGCC-3′. Behavioral tests were performed using the ZebraBox (Viewpoint) and its video quantification module, and sleep was defined as continuous inactivity for 60 s.

Human Genetic Data. A total of 19 sleep phenotypes and disorders GWAS summary statistics from the UK Biobank were included (Dataset S2). The genomic location of *MIR137* on chromosome 1 (98.453.556 to 98.515.419 [GRCh37/hg19]) was extended to an area 1 Mbp upstream and downstream. Genes in this area were selected from the GRCh37 genome assembly and their location marked by a blue rectangle. Any nonsignificant SNPs ($P \geq$ 5e-8) were plotted as gray dots, whereas significant SNPs with a $P \leq$ 5e-8 were plotted in dark red and labeled. Additionally, SNPs from the sleep duration GWAS ($P \leq$ 5e-2) were plotted in red.

Statistical Analysis. All statistical analyses were made using GraphPad Prism 8. Results were compared using Student's *t* test, one-way or two-way ANOVAs, or nonparametric Kruskal–Wallis test followed by multiple-comparison tests when pertinent. Statistical significance was expressed as follows: $*P < 0.05$, $**P < 0.01$, $***P < 0.001$, and $****P < 0.0001$.

Data Availability. Custom MATLAB (MathWorks) scripts used to process data have been deposited in GitHub (https://github.com/Bandarabadi/SleepZebrafish). Details regarding cell culturing, miRNA and mRNA analyses from cell culture and mouse brain, fluorescence in situ hybridization and immunohistochemistry, cytokine stimulations, and surgical procedures are described in *SI Appendix*. Previously published data were used for this work (38, 39, 40).

ACKNOWLEDGMENTS. We are especially grateful to Thi Cam Ha Nguyen, Stine Christensen, Helle Kinggaard Lilja-Fischer, and Birte Kofoed for their technical assistance. We thank Professor Johan Jakobsson for the miR sponge constructs, Professor Luis De Lecea for the mmu-hypocretin promotor, and Professor Torben Ørntoft for providing the colorectal cancer cell lines. We acknowledge the Core Facility for Integrated Microscopy, Faculty of Health and Medical Sciences, University of Copenhagen. The Lundbeck Foundation – LF Fellowship (A.H., K.F.M., J.L.J., and B.R.K.). We also thank The Lundbeck Foundation (R165-2013-15524 [A.H.] and R77-A6365 [A.S.]), Carlsberg Foundation Young Researcher Fellowship (J.L.J. and B.R.K.), The Foundation for Research in Neurology R25-A763 (A.H.), The Swiss NSF (A.A.; 31003A_173126 [M.T.], 190605 [M.B.], and 188789 [F.A.]), and European Research Council (A.A.).

Author affiliations: [a]Department of Clinical Biochemistry, Molecular Sleep Laboratory, Rigshospitalet, 2600 Glostrup, Denmark; [b]Department of Clinical Medicine, Center for RNA Medicine, Aalborg University, 2450 Copenhagen, Denmark; [c]Department of Biomedical Sciences, Faculty of Biology and Medicine, University of Lausanne, 1005 Lausanne, Switzerland; [d]Department of Public Health, Section for Epidemiology, University of Copenhagen, 1356 Copenhagen, Denmark; [e]Department of Neuroscience, University of Copenhagen, 2200 Copenhagen, Denmark; [f]Department of Neurology, Center for Experimental Neurology, University of Bern, Inselspital University Hospital Bern, 3010 Bern, Switzerland; [g]Department of Biomedical Research, University of Bern, Inselspital University Hospital Bern, 3008 Bern, Switzerland; [h]Department of Cellular and Molecular Medicine, Faculty of Health and Medical Sciences, University of Copenhagen, 2200 Copenhagen, Denmark; and [i]Lyon Neurosciences Research Center, INSERM U, CNRS UMR 5292, University Lyon 1, 69500 Bron, France

Author contributions: A.H. conceived the study with important input from B.R.K.; A.H., A.A., M.T., and B.R.K. designed research; A.H., M.-L.P., K.F.M., J.L.J., I.B., Y.A., and A.S. performed research; F.A., A.S., A.A., M.T., and B.R.K. contributed new reagents/analytic tools; A.H., M.-L.P., M.B., K.F.M., J.L.J., R.L., Y.A., F.A., A.S., M.J., M.T., and B.R.K. analyzed data; and A.H., M.-L.P., M.B., M.T., and B.R.K. wrote the paper.

1. L. de Lecea *et al.*, The hypocretins: Hypothalamus-specific peptides with neuroexcitatory activity. *Proc. Natl. Acad. Sci. U.S.A.* **95**, 322–327 (1998).
2. T. Sakurai *et al.*, Orexins and orexin receptors: A family of hypothalamic neuropeptides and G protein-coupled receptors that regulate feeding behavior. *Cell* **92**, 573–585 (1998).
3. J. L. Justinussen, A. Holm, B. R. Kornum, An optimized method for measuring hypocretin-1 peptide in the mouse brain reveals differential circadian regulation of hypocretin-1 levels rostral and caudal to the hypothalamus. *Neuroscience* **310**, 354–361 (2015).
4. B. Y. Mileykovskiy, L. I. Kiyashchenko, J. M. Siegel, Behavioral correlates of activity in identified hypocretin/orexin neurons. *Neuron* **46**, 787–798 (2005).
5. A. Vassalli, P. Franken, Hypocretin (orexin) is critical in sustaining theta/gamma-rich waking behaviors that drive sleep need. *Proc. Natl. Acad. Sci. U.S.A.* **114**, E5464–E5473 (2017).
6. S. Nishino, B. Ripley, S. Overeem, G. J. Lammers, E. Mignot, Hypocretin (orexin) deficiency in human narcolepsy. *Lancet* **355**, 39–40 (2000).
7. R. M. Chemelli *et al.*, Narcolepsy in orexin knockout mice: Molecular genetics of sleep regulation. *Cell* **98**, 437–451 (1999).
8. A. R. Adamantidis, F. Zhang, A. M. Aravanis, K. Deisseroth, L. de Lecea, Neural substrates of awakening probed with optogenetic control of hypocretin neurons. *Nature* **450**, 420–424 (2007).
9. C. J. Winrow, J. J. Renger, Discovery and development of orexin receptor antagonists as therapeutics for insomnia. *Br. J. Pharmacol.* **171**, 283–293 (2014).
10. S. Tanaka, Transcriptional regulation of the hypocretin/orexin gene. *Vitam. Horm.* **89**, 75–90 (2012).
11. S. K. Fineberg, K. S. Kosik, B. L. Davidson, MicroRNAs potentiate neural development. *Neuron* **64**, 303–309 (2009).
12. S. Siegert *et al.*, The schizophrenia risk gene product miR-137 alters presynaptic plasticity. *Nat. Neurosci.* **18**, 1008–1016 (2015).
13. M. Alvarez-Saavedra *et al.*, miRNA-132 orchestrates chromatin remodeling and translational control of the circadian clock. *Hum. Mol. Genet.* **20**, 731–751 (2011).
14. C. J. Davis *et al.*, MicroRNA 132 alters sleep and varies with time in brain. *J. Appl. Physiol. (1985)* **111**, 665–672 (2011).
15. E. Cummings *et al.*, Mood congruent psychotic symptoms and specific cognitive deficits in carriers of the novel schizophrenia risk variant at MIR-137. *Neurosci. Lett.* **532**, 33–38 (2013).
16. M. Strazisar *et al.*, MIR137 variants identified in psychiatric patients affect synaptogenesis and neuronal transmission gene sets. *Mol. Psychiatry* **20**, 472–481 (2015).
17. E. Mahmoudi, M. J. Cairns, MiR-137: An important player in neural development and neoplastic transformation. *Mol. Psychiatry* **22**, 44–55 (2017).
18. C. Wright *et al.*, Polymorphisms in MIR137HG and microRNA-137-regulated genes influence gray matter structure in schizophrenia. *Transl. Psychiatry* **6**, e724 (2016).
19. P. Mestdagh *et al.*, The microRNA body map: Dissecting microRNA function through integrative genomics. *Nucleic Acids Res.* **39**, e136 (2011).
20. S. Saxena, Z. O. Jónsson, A. Dutta, Small RNAs with imperfect match to endogenous mRNA repress translation. Implications for off-target activity of small inhibitory RNA in mammalian cells. *J. Biol. Chem.* **278**, 44312–44319 (2003).
21. J. J. Glascock *et al.*, Delivery of therapeutic agents through intracerebroventricular (ICV) and intravenous (IV) injection in mice. *J. Vis. Exp.* **56**, 2968 (2011).
22. Y. Yamamoto *et al.*, Postnatal development of orexin/hypocretin in rats. *Brain Res. Mol. Brain Res.* **78**, 108–119 (2000).
23. Y. Ogawa, T. Kanda, K. Vogt, M. Yanagisawa, Anatomical and electrophysiological development of the hypothalamic orexin neurons from embryos to neonates. *J. Comp. Neurol.* **525**, 3809–3820 (2017).
24. J. Dalal *et al.*, Translational profiling of hypocretin neurons identifies candidate molecules for sleep regulation. *Genes Dev.* **27**, 565–578 (2013).
25. P. Landgraf *et al.*, A mammalian microRNA expression atlas based on small RNA library sequencing. *Cell* **129**, 1401–1414 (2007).
26. R. D. Smrt *et al.*, MicroRNA miR-137 regulates neuronal maturation by targeting ubiquitin ligase mind bomb-1. *Stem Cells* **28**, 1060–1070 (2010).
27. M. Lagos-Quintana, R. Rauhut, W. Lendeckel, T. Tuschl, Identification of novel genes coding for small expressed RNAs. *Science* **294**, 853–858 (2001).
28. M. H. Willemsen *et al.*, Chromosome 1p21.3 microdeletions comprising DPYD and MIR137 are associated with intellectual disability. *J. Med. Genet.* **48**, 810–818 (2011).
29. P. Franken, D. J. Dijk, I. Tobler, A. A. Borbély, Sleep deprivation in rats: Effects on EEG power spectra, vigilance states, and cortical temperature. *Am. J. Physiol.* **261**, R198–R208 (1991).
30. I. Tobler, A. A. Borbély, Sleep EEG in the rat as a function of prior waking. *Electroencephalogr. Clin. Neurophysiol.* **64**, 74–76 (1986).
31. S. Tabuchi *et al.*, Conditional ablation of orexin/hypocretin neurons: A new mouse model for the study of narcolepsy and orexin system function. *J. Neurosci.* **34**, 6495–6509 (2014).
32. S. Zhan *et al.*, Tumor necrosis factor-alpha regulates the Hypocretin system via mRNA degradation and ubiquitination. *Biochim. Biophys. Acta* **1812**, 565–571 (2011).
33. N. S. Waleh, A. Apte-Deshpande, A. Terao, J. Ding, T. S. Kilduff, Modulation of the promoter region of prepro-hypocretin by alpha-interferon. *Gene* **262**, 123–128 (2001).
34. M. Utsuyama, K. Hirokawa, Differential expression of various cytokine receptors in the brain after stimulation with LPS in young and old mice. *Exp. Gerontol.* **37**, 411–420 (2002).
35. J. Giacomotto *et al.*, Developmental suppression of schizophrenia-associated miR-137 alters sensorimotor function in zebrafish. *Transl. Psychiatry* **6**, e818 (2016).
36. A. Chen *et al.*, QRFP and its receptors regulate locomotor activity and sleep in zebrafish. *J. Neurosci.* **36**, 1823–1840 (2016).
37. A. Seifinejad *et al.*, Molecular codes and in vitro generation of hypocretin and melanin concentrating hormone neurons. *Proc. Natl. Acad. Sci. U.S.A.* **116**, 17061–17070 (2019).
38. H. S. Dashti *et al.*, Genome-wide association study identifies genetic loci for self-reported habitual sleep duration supported by accelerometer-derived estimates. *Nat. Commun.* **10**, 1100 (2019).
39. S. E. Jones *et al.*, Genetic studies of accelerometer-based sleep measures yield new insights into human sleep behaviour. *Nat. Commun.* **10**, 1585 (2019).
40. A. Doherty *et al.*, GWAS identifies 14 loci for device-measured physical activity and sleep duration. *Nat. Commun.* **9**, 5257 (2018).
41. J. J. Crowley *et al.*, Disruption of the microRNA 137 primary transcript results in early embryonic lethality in mice. *Biol. Psychiatry* **77**, e5–e7 (2015).
42. Y. Cheng *et al.*, Partial loss of psychiatric risk gene Mir137 in mice causes repetitive behavior and impairs sociability and learning via increased Pde10a. *Nat. Neurosci.* **21**, 1689–1703 (2018).
43. A. L. Collins *et al.*, Transcriptional targets of the schizophrenia risk gene MIR137. *Transl. Psychiatry* **4**, e404 (2014).
44. T. W. Mi *et al.*, Loss of MicroRNA-137 impairs the homeostasis of potassium in neurons via KCC2. *Exp. Neurobiol.* **29**, 138–149 (2020).
45. J. M. Krueger, D. M. Rector, L. Churchill, Sleep and cytokines. *Sleep Med. Clin.* **2**, 161–169 (2007).
46. S. Su *et al.*, miR-142-5p and miR-130a-3p are regulated by IL-4 and IL-13 and control profibrogenic macrophage program. *Nat. Commun.* **6**, 8523 (2015).
47. S. O'Reilly, M. Ciechomska, N. Fullard, S. Przyborski, J. M. van Laar, IL-13 mediates collagen deposition via STAT6 and microRNA-135b: A role for epigenetics. *Sci. Rep.* **6**, 25066 (2016).
48. B. R. Kornum *et al.*, Narcolepsy. *Nat. Rev. Dis. Primers* **3**, 16100 (2017).
49. E. Postiglione *et al.*, Narcolepsy with intermediate cerebrospinal level of hypocretin-1. *Sleep (Basel)* **45**, zsab285 (2022).
50. B. R. Kornum, Narcolepsy type 1: What have we learned from immunology? *Sleep (Basel)* **43**, zsaa055 (2020).
51. K. E. Szulwach *et al.*, Cross talk between microRNA and epigenetic regulation in adult neurogenesis. *J. Cell Biol.* **189**, 127–141 (2010).
52. T. Matijevic, J. Knezevic, M. Slavica, J. Pavelic, Rett syndrome: From the gene to the disease. *Eur. Neurol.* **61**, 3–10 (2009).
53. J. Yin *et al.*, miR-137: A new player in schizophrenia. *Int. J. Mol. Sci.* **15**, 3262–3271 (2014).
54. M. T. Carter *et al.*, Hemizygous deletions on chromosome 1p21.3 involving the DPYD gene in individuals with autism spectrum disorder. *Clin. Genet.* **80**, 435–443 (2011).
55. D. Young *et al.*, Sleep problems in Rett syndrome. *Brain Dev.* **29**, 609–616 (2007).
56. S. Wilson, S. Argyropoulos, Sleep in schizophrenia: Time for closer attention. *Br. J. Psychiatry* **200**, 273–274 (2012).